

Effect of Injection Pressure and Timing of the Ternary Blends (Ethanol-Biodiesel-Diesel) on Combustion Characteristics

Sakda Thongchai, Ob Nilaphai and Manida Tongroon*

ATAE Research Unit, Department of Mechanical Engineering, Faculty of Engineering at Sriracha, Kasetsart University, Thailand

* Corresponding author, E-mail: manida@src.ku.ac.th

Received: 7 May 2023; Revised: 13 June 2023; Accepted: 15 June 2023

Online Published: 26 August 2023

Abstract: This research studies the combustion characteristics of a compression ignition engine when using ternary blends (ethanol-biodiesel-diesel). Because ethanol is renewable energy and can lower exhaust emissions, it is interesting to use in a diesel engine. With less effort to prepare the fuel and apply it in the engine, the blending technique is used in this research. However, phase separation readily occurs as the percentage of ethanol increases and at the low ambient temperature. Fortunately, biodiesel has been used commercially as a blend and can act as a surfactant to keep the phase stable. To comply with the market, the blend ratio used is B3E5, B7E5, and B10E10, where B stands for biodiesel, E is ethanol, and the numeric presents the percent of each fuel by volume. In addition, diesel adding 3 percent biodiesel as a lubricity enhancer is used as the reference. Combustion features such as heat release rate, ignition delay, and mass fraction burned derived from in-cylinder pressure are experimented with through a single-cylinder common-rail diesel engine. The injection pressure varies from 500, 700, and 1000 bar, while injection timing adjusts from 335, 340, 345, 350, and 355°CA. With ethanol concentration, the ignition commences earlier than diesel B3 due to the puffing phenomena. However, adding more biodiesel content results in later ignition because of the difficulty of the fuel-air mixing process. The high content of ethanol and biodiesel yields the lengthiest ignition delay.

Keywords: Ethanol; Biodiesel; Ternary blends; Diesohol



1. Introduction

Due to energy depletion and security problems, renewable fuels have been extensively investigated. Ethanol has successfully been applied in a spark ignition (SI) engine up to 85% blended with gasoline, even used in the neat form in Brazil [1]. On the other hand, biodiesel has been used in compression ignition (CI) engines as the commercial fuel in some countries but a limitation to 10-20% blended with diesel [2, 3]. Moreover, the air pollution problems specifically emit from a CI engine with high smoke and NO_x concentration. Alternative fuel is increasingly demanding, especially ethanol which can significantly reduce smoke emissions [4, 5].

However, applying ethanol in a CI engine requires tremendous effort than in SI because its properties significantly differ from diesel, such as cetane number. The promising approach to use in CI engines is the blending method. Nevertheless, ethanol could not be miscible into diesel without the solubility enhancer. Therefore, many additives have been studied such as Sorbitan Monooleate, polyoxymethylene dimethyl ethers, and n-butanol [6-8]. Biodiesel is a renewable fuel and already mixes with diesel in some countries. Moreover, the biodiesel amount could improve the solubility of ethanol-diesel blends and compensate for the blends' low density, viscosity, and lubricity properties [9-11]. Therefore, using biodiesel as a surfactant is interesting.

Due to the low heating value, previous researches found that fuel consumption increases when using ethanol-biodiesel-diesel blends [12, 13]. However, the tri-blends present an advantage over diesel in terms of thermal efficiency [14, 15]. Depending on the test condition, CO and HC emitted from ternary blends demonstrate inconclusive correlation compared to that of neat diesel fuel [16, 17]. The blends are likely to increase the NO_x concentration [18]. However, many researchers have proved that the smoke/particulate matter (PM) significantly decreases with the blends of ethanol/biodiesel [19-21]. For combustion characteristics, ethanol tends to retard the ignition, thus lengthening the ignition delay [22, 23]. Consequently, the heat release rate is high.

Although there is considerable research on ternary blends, the effect of injection pressure and timing on the Ethanol-Biodiesel-Diesel blend used in the common rail diesel engine at medium operating condition is limited. Moreover, the ratio of ethanol and biodiesel in this research is highly promising because the amount of biodiesel blended is commercially used in many countries. This paper has also compared the effect of ethanol and biodiesel solely. In the meantime, the combined influence has been evaluated. The effect of injection timing is presented first, followed by the injection pressure. The influence of fuel properties has been demonstrated in the last section.



2. Apparatus

2.1 Engine

An agricultural base single cylinder four stroke diesel engine with a naturally aspirated intake system and water cooling was used throughout this study. The fuel is injected directly into the combustion chamber via a high-pressure common rail system. An in-house electronic injection system controls the injection timing and duration. The engine specification is detailed in Table 1.

2.2 Test Fuel

The ternary blends were prepared in two steps, shown in Fig. 1. Firstly, biodiesel was mixed with diesel called BX, where X is the percentage of biodiesel. This study chose B3, B7 and B10 to imitate commercial use. Then, ethanol was blended into BX, named BXEY, where Y is the percentage of ethanol in BX. Only 5% and 10% ethanol were selected to blend to prevent phase separation.

Therefore, the final blends include B3E5, B7E5, and B10E10. Also, B3 was tested as the reference. The fuel properties and the amount of biodiesel and ethanol are presented in Table 2.

Table 1 Engine specification

Specification	
Engine type	A horizontally single-cylinder four- stroke engine
Displacement volume	709 cm ³
Bore x Stroke	97 x 96 mm.
Compression ratio	18:1
No. intake valve	1
No. exhaust valve	1
Injection system	Electronic common rail
Cooling system	Liquid-cooled
Max power	10.3 kW at 2400 rpm
Max torque	49 Nm at 1600 rpm

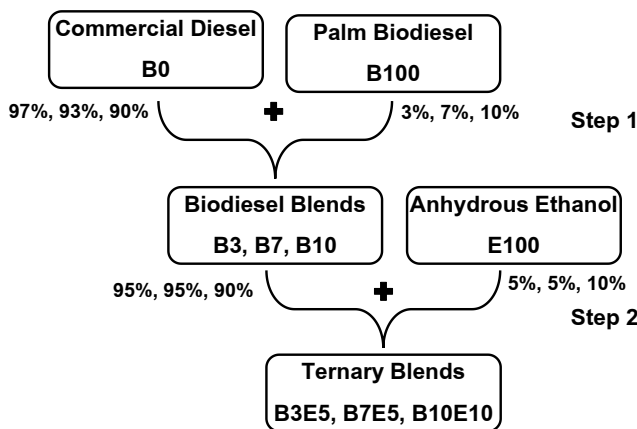


Fig. 1 Procedure of fuel preparation

**Table 2 Fuel Properties**

Properties	B3E5	B7E5	B10E10	Diesel (B3)	Ethanol	Biodiesel
Ethanol (%)	5	5	10	0	100	0
Biodiesel (%)	2.85	6.65	9	3	0	100
Diesel (%)	92.15	88.35	81	100	0	0
Density (g/cm ³)	0.814	0.816	0.815	0.832	0.786	0.868
Viscosity (cSt)	3.0	3.0	2.8	3.9	1.2	4.5
Heating value (MJ/kg)	43.9	42.9	41.7	45.05	27.6	40.1
Cetane number	56.5	56.7	53.6	-	-	67.9
Heat of vaporization (kJ/kg)				254 [25]	904 [25]	254 [25]
Enthalpy of vaporization (kJ/g)				0.250 [26]	0.846 [27]	0.245 [26]
Specific heat capacity (J g ⁻¹ K ⁻¹) @298 K				1.87-1.92 [27]	2.44 [28]	2.12 [29]

2.3 Combustion analysis

The engine speed was controlled at 1600 rpm and load at brake mean effective pressure (BMEP) of 5 bar by a prony brake dynamometer, measured the loading force by S-type tension/ compression load cell with the capability of 1961 N from Minebea, model U3B1-200K-B. The schematic diagram of the experimental system is presented in Fig. 2. The combustion behaviors were analyzed through in-cylinder pressure data acquired by a Kistler model 6052C piezoelectric pressure transducer. One hundred consecutive cycles triggered every 0.1-degree crank angle by an Autonics model E40HB6-3600-3-T-24 encoder were amplified by a Kistler model 5108 charge amplifier before being recorded by an in-house LabVIEW base program. The average in-cylinder pressure

value was used to calculate the heat release rate in Eq. (1), specified by Heywood [30].

$$\frac{dQ}{d\theta} = \frac{\gamma}{\gamma - 1} p \frac{dV}{d\theta} + \frac{1}{\gamma - 1} V \frac{dp}{d\theta} \quad (1)$$

Where V is cylinder volume, p is averaged in-cylinder pressure, and γ is the ratio of specific heat, equal to 1.3 for this study.

The engine was warmup until the lubricant and coolant water reached 80°C before the test started. The injection timings were varied from 335°CA to 355°CA with the 5°CA increment at the fixed injection pressure of 700 bar. On the other hand, the injection pressure was tested at 500, 700 and 1000 bar when the injection timing was controlled at 345°CA. All test fuels were tested and compared with the same conditions.

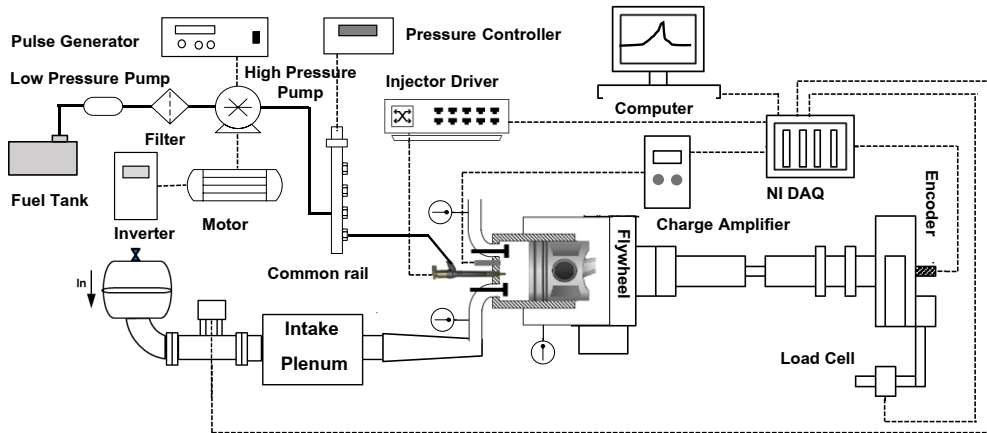


Fig. 2 Schematic diagram of experimental setup

3. Result and Discussion

3.1 Effect of Injection Timing

Fig. 3 presents the effect of injection timing on the heat release rate of (a) B3, (b) B3E5, (c) B7E5, and (d) B10E10, respectively. The start of combustion is defined as the crank angle where the percentage of fuel burnt is 5%. The ignition delay is the interval between the injection timing and the start of combustion. Fundamentally, when the fuel injection commences early, the liquid fuel can atomize, vaporize, and mix with air, preparing for ignition early. Therefore, all test fuels exhibited the same trend where the earlier the injection, the auto-ignition started earlier.

The ignition timing retardation is not at the same interval as injection timing retardation at the very early injection. For example, at the injection timing of 335°CA, the ignition occurred at 349°CA for B3; when the injection was delayed to 340°CA, the ignition retarded about 2.8°CA less than 5°CA of the

delayed injection. However, the ignition timing intervals extended and were equivalent to the injection retardation intervals when the injection timing closed to the top dead center for all test fuels, shown in Fig.4.

Not only the ignition happened early with the early injection, but 10% and 50% of mass burnt also (Fig.4). Nevertheless, there is no certain trend of 90% mass burnt (the combustion finished). At injection timing of 340 and 345°CA, the combustion seems to terminate earlier than 335°CA, the earliest injection timing. The low air temperature and pressure at the early injection are the causes. Moreover, the injected fuel hardly vaporizes and oxidizes. Therefore, the ignition delay is the lengthiest at the earliest injection timing and decreases with the retardation, as presented in Fig.5. With the lengthening ignition delay, more fuel accumulates before the oxidation occurs, thus releasing greater heat in Fig. 6.



บทความวิจัย

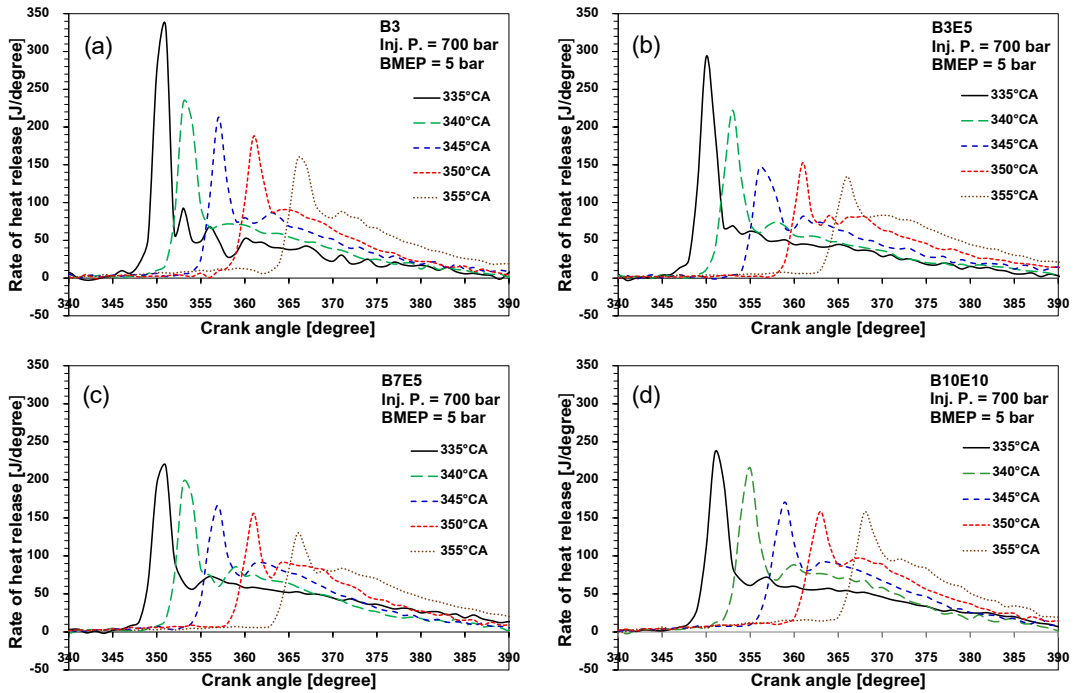


Fig. 3 Heat release rate of (a) B3, (b) B3E5, (c) B7E5, and (d) B10E10 when varying injection timing

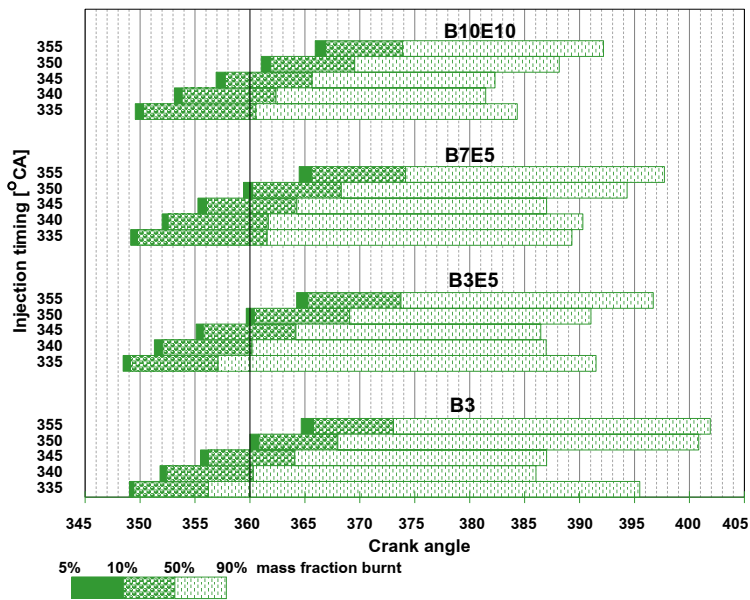


Fig. 4 The effect of injection timing on combustion phasing

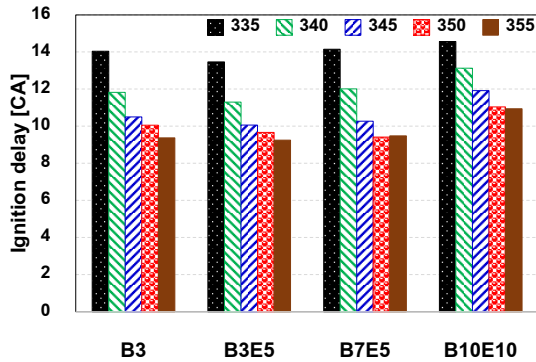


Fig. 5 The effect of varying injection timing on ignition delay

Interestingly, the effect of injection timing on the burning rate during premixed (5-50% mass burnt in Fig.7) is not the same among all test fuels. With the lower amount of oxygenated fuels (B3 and B3E5), the burning rate during premixed combustion decreases when the injection timing retards and vice versa for the higher blended ratio of alternative fuel (B7E5 and B10E10). When injection timing lately happens, the ignition delay decreases, thus reducing the accumulated premixed mixture to combust during the rapid combustion phase [31]. Therefore, the rate of combustion reduces. Although the ignition delay also lessens for the B7E5 and B10E10, high oxygen molecules enhance the air-fuel mixture process. In addition, high air temperature during the late injection accelerates the burning rate. Not shown here, there is no correlation between the diffusion combustion (50-90% mass burnt) with the injection timing.

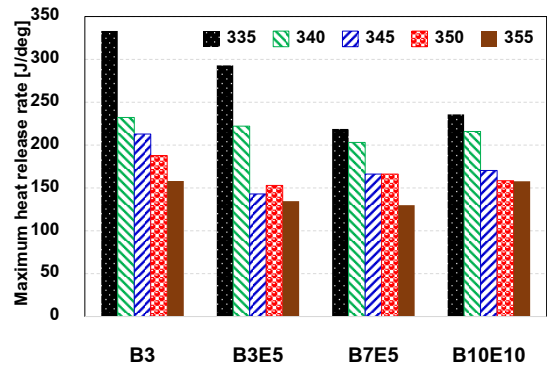


Fig. 6 The effect of varying injection timing on the maximum heat release rate.

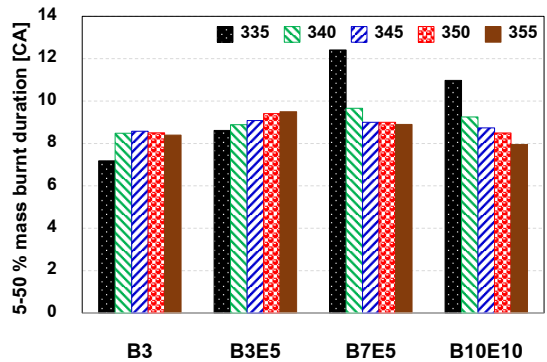


Fig. 7 The duration to burn 5-50% mass when varying injection timing.

3.2 Effect of Injection Pressure

The effect of varying injection pressure at 500, 700, and 1000 bar on the heat release rate when using (a) B3, (b) B3E5, (c) B7E5, and (B10E10) is exhibited in Fig. 8, respectively. It shows that the ignition starts early with a high heat release rate when the injection pressure increases. It indicates that the high injection pressure results in the shortening ignition delay in

Fig. 9 but release high heat even though less time is available for fuel accumulated. The injected fuel readily atomizes into the fine droplet with increased injection pressure [32]. Tiny fuel drops could vaporize and mix with air quickly. Consequently, the auto-ignition is achieved early. Moreover, the mass fuel injection rate increases with the high injection pressure [33]. Therefore, more fuel oxidizes and releases heat during the premixed combustion mode.

Better fuel atomization at the high injection pressure accelerates the ignition and the burning rate during the premixed combustion phase, illustrated in Fig. 10 for all test fuels. Also, for the combustion duration in Fig. 11 (5-90% mass burnt), all test fuels consume lesser time with the increased injection pressure.

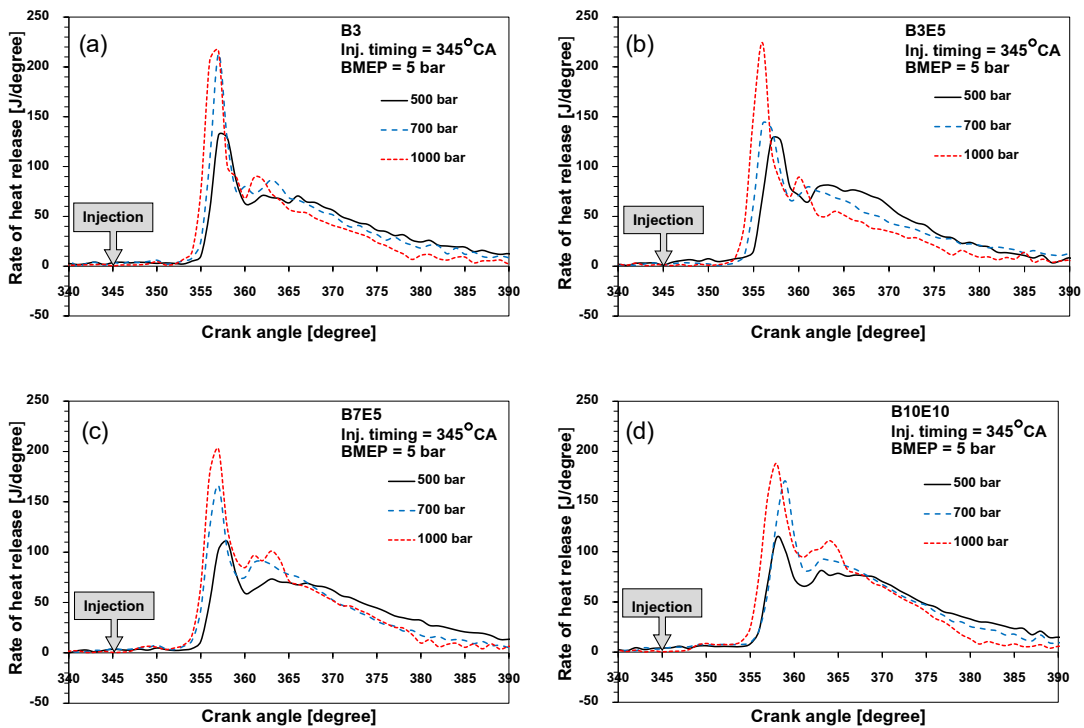


Fig. 8 Heat release rate of (a) B3, (b) B3E5, (c) B7E5, and (d) B10E10 when varying injection pressure

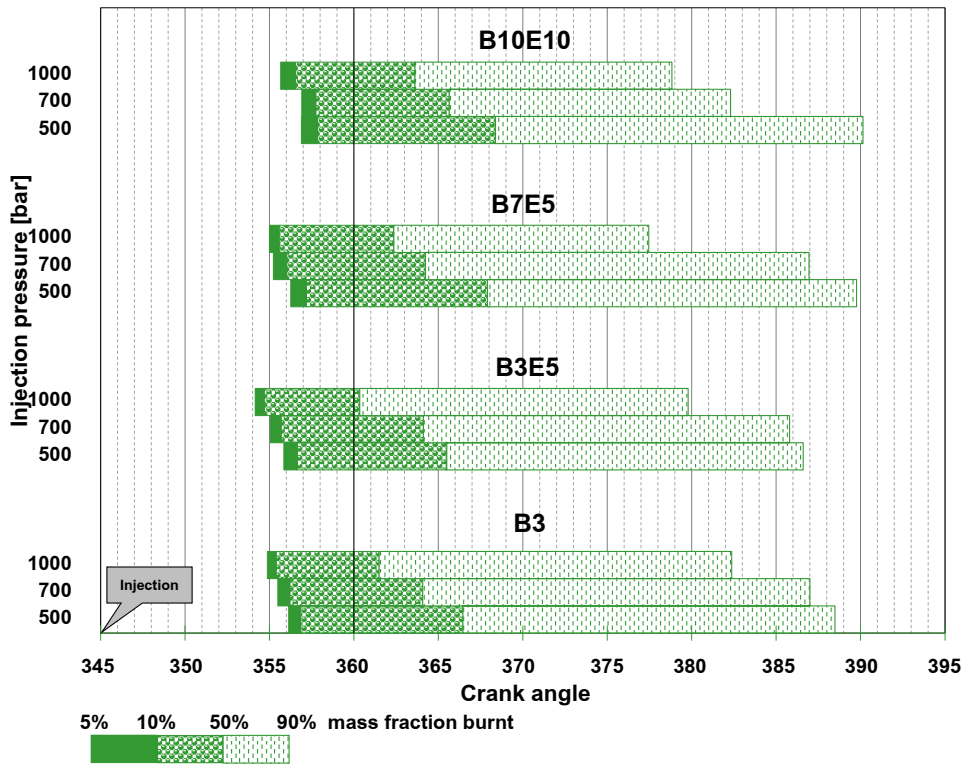


Fig. 9 5, 10, 50 and 90% mass fraction burnt and the location happening when varying injection pressure

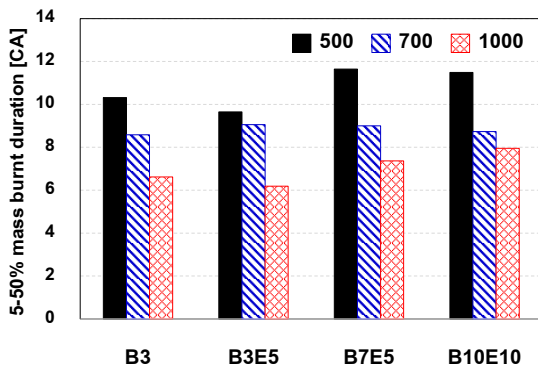


Fig. 10 The duration to burnt 5-50% mass when varying injection pressure

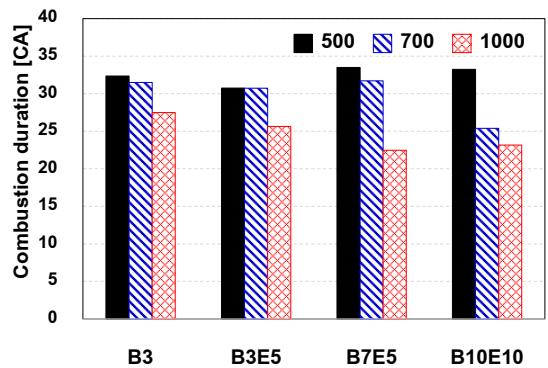


Fig. 11 The combustion duration when varying injection pressure

3.3 Effect of fuel properties

Fig. 12 compares the heat release rate of B3, B3E5, B7E5, and B10E10 at the injection pressure of 700 MPa and the injection timing of 340°CA. Although the results of other test conditions are not shown here, the trend is the same. To characterize the sole effect of ethanol, B3 and B3E5 are considered. The result indicates that increasing 5% ethanol into the blend accelerates self-ignition over B3. The shortening ignition delay is clearly presented in Fig. 13. The results contradict many previous studies where ethanol retard the auto-ignition [22, 23]. The puffing phenomenon is the cause [34]. Although the appearance of the blend is a transparent homogeneous solution, ethanol as sub-droplets is diffused and surrounded by the droplet of diesel and biodiesel. With low boiling temperatures, ethanol first vaporizes and forms a bubble inside the droplets after the atomized fuels are heated. Those bubbles expand outward and drive the surrounding high boiling point droplet, rupturing and pushing the vapor jet. This incident is called the puffing phenomenon and leads to secondary atomization, which could accelerate auto-ignition.

The specific effect of biodiesel in the blend is clarified by comparing B3E5 and B7E5. Adding only 3.8% biodiesel could delay the ignition. The puffing incident is abated with biodiesel content [35]. Secondary atomization barely induces.

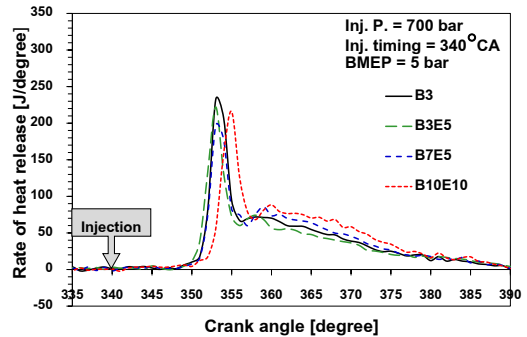


Fig. 12 The effect of fuel properties (B3, B3E5, B7E5, and B10E10) on Heat release rate

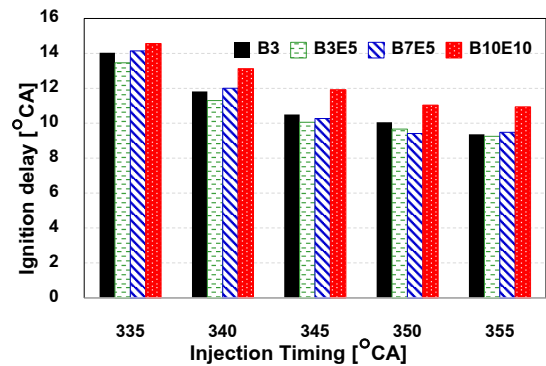


Fig. 13 The effect of test fuel on the ignition delay at any injection timing

Moreover, the atomization of viscous and high-density fuel is difficult. Therefore, the fuel hardly vaporizes. The fuel-air mixing process is hindered. Consequently, the ignition delay is lengthened.

The effect of ethanol combined with biodiesel is investigated through the B10E10 fuel. The high percentage of ethanol and biodiesel prolongs the ignition delay the most among all test fuels. The cooling effect resulted from the high heat of



vaporization and enthalpy of vaporization in Table 2 of high ethanol content dominates in this case. In addition, the difficulty of fuel atomization and vaporization of biodiesel also contribute.

The maximum heat release rate of all test fuels at all injection timings is illustrated in Fig. 14. The peak heat release does not correlate with the ignition delay, where the higher heat happens with the lengthener ignition delay. B3, with the highest heating value, releases the utmost heat, although the ignition delay is short. The maximum heat release rate of all ethanol blends is lower than diesel. The low heating value of ethanol is one vital cause. However, the long ignition delay of B10E10 coupled with the high air-fuel mixing process increases the rate of heat release over B7E5 and even B3E5 sometimes.

The combustion phasing from 5-50% mass burnt (premixed combustion) of all test fuels is presented in Fig. 15. At early injection timing (335-340°CA), B3 combusts the fastest, followed by B3E5, B10E10, and B7E5 during premixed combustion. The rate of oxidation seems to depend on the heating value of fuels. When the heating value is lower, more blend is required to deliver the same BMEP. Therefore, more time is needed to combust, hence slow burning in terms of time scale base. Even though more B10E10 necessitates, the premixed combustion rate looks faster than B7E5. Because of the lengthy ignition

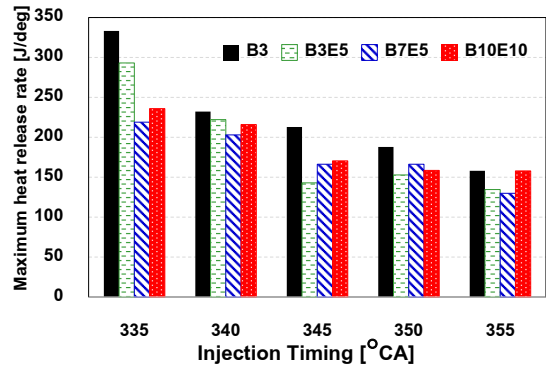


Fig. 14 The effect of test fuel on the maximum heat release rate at any injection timing

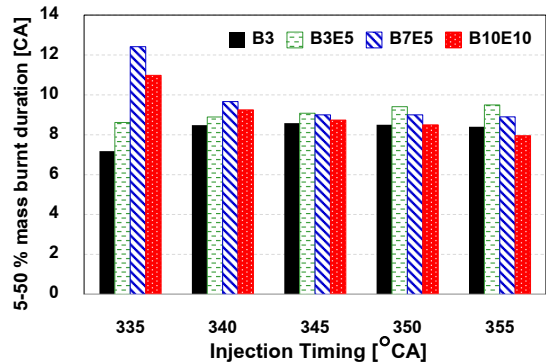


Fig. 15 5-50% mass burnt duration of B3, B3E5, B7E5, and B10E10 at injection pressure of 700 bar and varying injection timing

delay of B10E10, much more accumulated fuel-air mixture oxidizes once the ignition happens. Rapid oxidation, as seen in a higher maximum heat release rate, consumes the charge mixture and results in faster burning than B7E5.

At the late injection, the effect of high oxygen content dominates the burning rate, as previously described. The fuel-air mixing process is enhanced



for B10E10 and B7E5 fuel, leading to faster burn than B3E5. Moreover, B10E10 sometimes indicates more rapid combustion than B3 (at 355°C injection timing).

4. Conclusion

The study investigates the effect of injection timing and pressure on the combustion characteristics of ternary blends (B3, B3E5, B7E5, and B10E10). Moreover, the influence of ethanol and biodiesel concentration is presented separately. The combined effect of ethanol and biodiesel is also exhibited. The conclusions are:

- The effects of injection timing on the combustion characteristics for all blends are the same. With the earlier injection timing, the ignition happens earlier with the extended ignition delay. Only the burning late during the premixed combustion phase differs, where the low-oxygenated blends combust slowly while high-content oxygen fuel oxidizes at the late injection.
- Better fuel atomization resulting from the high injection pressure leads to early ignition timing, shortened ignition delay, and fast burning for all blends.
- Ethanol content in the blends with less biodiesel concentration could induce the puffing phenomena, leading to the second atomization and shortening ignition delay.
- Biodiesel content in the ternary blends could suppress the puffing incident. Moreover, the

difficulty of its atomization and vaporization retards the ignition.

- The high heat of vaporization of ethanol combined with the difficulty of atomization/vaporization of biodiesel significantly delay the ignition. However, with the high oxygen content, the burning rate at the premixed combustion phase is enhanced when the injection commences late.

5. Acknowledgement

This research was financially supported by Kasetsart University Research and Development Institute, KURDI (R-M 50.64), Thailand.

6. References

- [1] J. Mączyńska, M. Krzywonos, A. Kupczyk, K. Tucki, M. Sikora, H. Pińkowska, A. Bączyk and I. Wielewska, Production and use of biofuels for transport in Poland and Brazil – The case of bioethanol, *Fuel*, 2019, 241, 989-996.
- [2] <https://www.eia.gov/energyexplained/biofuels/biodiesel-rd-other-use-supply.php>. (Accessed on 22 April 2023)
- [3] Sahara, A. Dermawan, S. Amaliah, T. Irawan and S. Dilla, Economic impacts of biodiesel policy in Indonesia: A computable general equilibrium approach, *Economic Structures*, 2022, 11, 22.



- [4] X. Wang, C. Geng, J. Dong, X. Li, T. Xu, C. Jin, H. Liu and B. Mao, Effect of diesel/PODE/ethanol blends coupled pilot injection strategy on combustion and emissions of a heavy duty diesel engine, *Fuel*, 2023, 335, 127024.
- [5] J. Lee, S. Lee and S. Lee, Experimental investigation on the performance and emissions characteristics of ethanol/diesel dual-fuel combustion, *Fuel*, 2018, 220, 72-79.
- [6] M.A. Shaikh and V. R. Patel, Experimental studies on ethanol solubility and nanoparticle (NP) stability in diesel fuel, *Chemical Engineering Research and Design*, 2022, 188,105-129.
- [7] C. Jin, X. Zhang, X. Wang et al., Effects of polyoxymethylene dimethyl ethers on the solubility of ethanol/diesel and hydrous ethanol/diesel fuel blends, *Energy Science and Engineering*, 2019, 7, 2855-2865.
- [8] C. Jin, X. Zhang, Z. Geng, X. Pang, X. Wang, J. Ji, G. Wang and H. Liu, Effects of various co-solvents on the solubility between blends of soybean oil with either methanol or ethanol, *Fuel*, 2019, 244, 461-471.
- [9] N. Kumar, R. Koul and R.C. Singh, Comparative analysis of ternary blends of renewable Diesel, diesel and ethanol with diesel, *Sustainable Energy Technologies and Assessments*, 2022, 50, 101828.
- [10] S. Pinzi, I. López, D.E. Leiva-Candia, M.D. Redel-Macías, J.M. Herreros, A. Cubero-Atienza and M.P. Dorado, Castor oil enhanced effect on fuel ethanol-diesel fuel blend properties, *Applied Energy*, 2018, 224, 409-416.
- [11] S. Madiwale, A. Karthikeyan and V. Bhojwani, Properties investigation and performance analysis of a diesel engine fuelled with Jatropa, Soybean, Palm and Cottonseed biodiesel using ethanol as an additive, *Materials Today: Proceedings*, 2018, 5(1), 657–664.
- [12] M. Vergel-Ortega, G. Valencia-Ochoa and J. Duarte-Forero, Experimental study of emissions in single-cylinder diesel engine operating with diesel-biodiesel blends of palm oil-sunflower oil and ethanol, *Case Studies in Thermal Engineering*, 2021, 26, 101190.



- [13] V. Kulanthaivel, A. Jayaraman, T. Rajamanickam and S. Selvam, Impact of diesel-algae biodiesel-anhydrous ethanol blends on the performance of CI engines, *Journal of Cleaner Production*, 2021, 295, 126422.
- [14] M.M. El-Sheekh, M.Y. Bedaiwy, A.A. El-Nagar, M. ElKelawy and H.A. Bastawissi, Ethanol biofuel production and characteristics optimization from wheat straw hydrolysate: Performance and emission study of DI-diesel engine fueled with diesel/biodiesel/ethanol blends, *Renewable Energy*, 2022, 191, 591-607.
- [15] H.V. Srikanth, Sharanappa G, B. Manne and S. Bharath Kumar, Niger seed oil biodiesel as an emulsifier in diesel-ethanol blends for compression ignition engine, *Renewable Energy*, 2021, 163, 1467-1478.
- [16] T. Prakash, V. Edwin Geo, L.J. Martin and B. Nagalingam, Effect of ternary blends of bio-ethanol, diesel and castor oil on performance, emission and combustion in a CI engine, *Renewable Energy*, 2018, 122, 301-309.
- [17] S.N. Bhat, S. Shenoy and P. Dinesha, Effect of bio-ethanol on the performance and emission of a biodiesel fueled compression ignition engine, *MATEC Web of Conferences*, 2018, 144, 04017.
- [18] D. Qi, L. Ma, R. Chen, X. Jin and M. Xie, Effects of EGR rate on the combustion and emission characteristics of diesel-palm oil-ethanol ternary blends used in a CRDI diesel engine with double injection strategy, *Applied Thermal Engineering*, 2021, 199, 117530.
- [19] J. Cong Ge, G. Wu, B. Yoo and N. Jung Choi, Effect of injection timing on combustion, emission and particle, morphology of an old diesel engine fueled with ternary blends at low idling operations, *Energy*, 2022, 253, 124150.
- [20] L. Zuo, J. Wang, D. Mei, S. Dai and D. Adu-Mensah, Experimental investigation on combustion and (regulated and unregulated) emissions performance of a common-rail diesel engine using partially hydrogenated biodiesel-ethanol-diesel ternary blend, *Renewable Energy*, 2022, 185, 1272-1283.
- [21] P. Karin, A. Tripatara, P. Wai, B. Oh, C. Charoenphonphanich, N. Chollacoop and H. Kosaka, Influence of ethanol-biodiesel blends on diesel engines combustion behavior and particulate matter physicochemical characteristics, *Case Studies in Chemical and Environmental Engineering*, 2022, 6, 100249.



- [22] S. Shamun, G. Belgiorno, G.D. Blasio, C. Beatrice and M. Tuner, Performance and emission of diesel-biodiesel-ethanol blends in a light duty compression ignition engine, *Applied Thermal Engineering*, 2018, 145, 444-452.
- [23] M. Mukhtar, F.Y. Hagos, A.R.A. Aziz, A.A. Abdullah and Z.A.A. Karim, Combustion characteristics of tri-fuel (diesel-ethanol-biodiesel) emulsion fuels in CI engine with micro-explosion phenomenon attributes, *Fuel*, 2022, 312, 122933.
- [24] M.J. Troughton, *Handbook of plastics joining: A practical guide*, 2nd Ed., William Andrew Inc., NY, USA, 2018.
- [25] J. Barata, Modelling of biofuel droplets dispersion and evaporation, *Renewable Energy*, 2008, 33, 769-779.
- [26] S. Sundarapandian, Performance and emission analysis of biodiesel operated CI engine, *Journal of Engineering, Computing and Architecture*, 2007, 1(2), 1–22.
- [27] A. Zanier and HW. Jäckle, Heat capacity measurements of petroleum fuels by modulated DSC, *Thermochemica Acta*, 1996, 287(2), 203–212.
- [28] NIST Standard Reference Database Number 69, Chemistry webbook, Standard Reference Data Program, National Institute of Standards and Technology (NIST), 2016.
- [29] W.M. Haynes, *Handbook of chemistry and physics*, Taylor and Francis Group, Boca Raton, FL, USA, 2015–2016, pp. 7-9.
- [30] J.B. Heywood, *Internal combustion engine fundamentals*, McGraw-Hill Inc, NY, USA, 1988.
- [31] Z. Huang, H. Lu, D. Jiang, K. Zeng, B. Liu, J. Zhang and X. Wang, Combustion behaviors of a compression-ignition engine fuelled with diesel/methanol blends under various fuel delivery advance angles, *Bioresource Technology*, 2004, 95, 331-341.
- [32] F. Juric, Z. Petranovic, M. Vujanovic, T. Katrasnik, R. Vihar, X. Wang and N. Duic, Experimental and numerical investigation of injection timing and rail pressure impact on combustion characteristics, *Energy Conversion and Management*, 2019, 185, 730-739.
- [33] R. Payri, G. Bracho, J.A. Soriano, P. Fernández-Yáñez and O. Armas, Nozzle rate of injection estimation from hole to hole momentum flux data with different fossil and renewable fuels, *Fuel*, 2020, 279, 118404.



- [34] Z. Wang, S. Wu, Y. Huang, S. Huang, S. Shi, X. Cheng and R. Huang, Experimental investigation on spray, evaporation and combustion characteristics of ethanol-diesel, water-emulsified diesel and neat diesel fuels, *Fuel*, 2018, 231, 438-448.
- [35] A. M. Faik and Y. Zhang, Multicomponent fuel droplet combustion investigation using magnified high speed backlighting and shadowgraph imaging, *Fuel*, 2018, 221, 89-109.